Research Square

Preprints are preliminary reports that have not undergone peer review.
They should not be considered conclusive, used to inform clinical practice,
or referenced by the media as validated information.

Efficiency and Mechanism of Lanthanum-Modified Red Clay for Sequestering Tungsten in Lake Sediments

Hanxiao Wang
Nanjing Institute of Environmental Sciences
Jiabao Yan
Nanjing Institute of Environmental Sciences
Li Zhou
Nanjing Institute of Environmental Sciences
Dongdong Zhu
Nanjing Institute of Environmental Sciences
Qi Li
Inner Mongolia University of Science and Technology
Yan Wang
Nanjing Institute of Environmental Sciences
Jing Xiao
Nanjing Institute of Environmental Sciences
Lan Zhang
Nanjing Institute of Environmental Sciences
Xiaohui You
Nanjing Institute of Environmental Sciences
Xiang Chen
Nanjing Institute of Environmental Sciences
Xiaoshuai Hang
hangxiaoshuai@163.com

Nanjing Institute of Environmental Sciences

Research Article

Keywords: LaRC, tungsten, sediment capping, Fe(III)/Mn(IV) hydroxides

Posted Date: June 1st, 2026

DOI: https://doi.org/10.21203/rs.3.rs-9555628/v1

License: This work is licensed under a Creative Commons Attribution 4.0 International License.
Read Full License

Additional Declarations: No competing interests reported.

Version of Record: A version of this preprint was published at Journal of Soils and Sediments on July 14th, 2026. See the published version at https://doi.org/10.1007/s11368-026-04463-x.

Efficiency and Mechanism of Lanthanum-Modified Red Clay for Sequestering Tungsten in Lake Sediments

Hanxiao Wang[a,1], Jiabao Yan [a,1], Li Zhou[a], Dongdong Zhu[a], Qi Li[b], Yan Wang[a], Jing Xiao[a], Lan Zhang[a], Xiaohui You[a], Xiang Chen[a, *], Xiaoshuai Hang [a, *]

[a.] Nanjing Institute of Environmental Sciences, Ministry of Ecology and Environment, Nanjing, 210042, China;

[b.] School of Energy and Environment, Inner Mongolia University of Science & Technology, Baotou,014010, China.

[1] These authors contributed equally to the paper.

*** Corresponding author:**

Name: Xiang Chen, **Xiaoshuai Hang**

E-mail address: cx13917094309@163.com, hangxiaoshuai@163.com

Abstract

Purpose This study developed a lanthanum-modified red clay (LaRC) to inhibit tungsten (W) release from contaminated lake sediments, and investigated its immobilization efficiency and underlying mechanisms compared to unmodified red clay (RC).

Materials and methods LaRC was synthesized via a liquid-phase method. Batch adsorption isotherms were fitted using Langmuir, Freundlich, and D-R models. Sediment cores from Yangcheng Lake were capped with RC or LaRC in a controlled incubation experiment. Dissolved oxygen (DO) and pH were measured by microelectrodes; soluble W, Fe(II), and Mn in porewater were analyzed using HR-Peeper and ICP-MS. X-ray photoelectron spectroscopy (XPS) and sequential extraction were employed to characterize geochemical fractions and binding mechanisms.

Results and discussion LaRC exhibited a higher maximum W adsorption capacity (83.94 mg g^{-1}) than RC (54.73 mg g^{-1}). LaRC capping reduced soluble W concentrations in porewater by 56.1% and diffusive flux by 0.98 $\mu g\, m^{-2}\, d^{-1}$, outperforming RC. XPS and D-R model analyses revealed that LaRC immobilizes W via formation of stable La–W precipitates (like $La_2(WO_4)_3$), whereas RC relies on adsorption onto Fe(III)/Mn(IV) hydroxides. The La–W precipitates remained stable even under reducing conditions, as evidenced by decoupled trends of rising soluble Fe(II)/Mn and declining W under LaRC treatment.

Conclusions LaRC capping effectively suppresses sedimentary W release by converting labile W into stable La–W precipitates. With higher adsorption capacity and better remediation performance than existing materials, LaRC offers a promising approach for managing tungsten contamination in aquatic sediments.

Keywords: LaRC; tungsten; sediment capping; Fe(III)/Mn(IV) hydroxides

1 Introduction

Tungsten was originally regarded as non-toxic and insoluble, leading to its widespread application in industrial production and national defense (Gold et al. 2007; Bolt & Mann 2016; Bostick et al. 2018). However, recent studies have shifted this perception, demonstrating that W can be readily oxidized to form various oxyanions such as WO_4^{2-}, which are mobile in soils and aquatic systems (Grant et al. 2021; Du et al. 2022). Evidence has accumulated regarding the adverse effects of W on human health, animals, plants, and microorganisms (Miller et al. 2001; Strigul et al. 2005; Adamakis et al. 2012; Kelly et al. 2013; Hadrup et al. 2022). Notably, epidemiological studies have suggested a potential association between elevated W levels in local dust and groundwater and the incidence of childhood leukemia in Nevada (Wasylenki et al. 2020). Consequently, W has been classified as an emerging contaminant of concern (Wasylenki et al. 2020). Regulatory measures have been implemented in some regions; for instance, regulatory limits for W in Russia have been set at 50 μg L^{-1} for drinking water reservoirs and 0.8 μg L^{-1} for fishery aquatic systems (Strigul 2010). Therefore, controlling W contamination in aquatic environments is crucial for ensuring drinking water safety and protecting the health of aquatic organisms.

Lake sediments act as significant sinks for heavy metals derived from water bodies (Miranda et al. 2021). These immobilized metals can be remobilized into the overlying water column under altered micro-interface conditions, posing potential threats to both ecological integrity and human health (Lin et al. 2024). For W, mobilization from sediments is primarily governed by factors such as temperature, pH, and the redox cycling of iron and manganese (Kashiwabara et al. 2013; Lin et al. 2024; Chen et al. 2025b). Elevated temperatures, acidic or alkaline pH shifts, and anaerobic conditions enhance W mobilization, primarily driven by the reductive dissolution of Fe(III)/Mn(IV) oxyhydroxides and competitive adsorption with dissolved organic matter (DOM) (Kashiwabara et al. 2013; Du et al. 2020; Lu et al. 2022; Xu et al. 2022; Lin et al. 2024; Chen et al. 2025b; Li et al. 2025). Previous

studies have shown the presence of W in sediments of lakes such as Taihu, Yangcheng, and Nansi (Guan et al. 2016; Wang et al. 2023; Chen et al. 2024b; Lin et al. 2024; Chen et al. 2025b). Notably, soluble W concentrations in the sediment pore water of Yangcheng Lake are reported to be higher than in other studied lakes (Chen et al. 2024b). Given that Yangcheng Lake is a major aquaculture base for hairy crab production (Wu et al. 2021), mitigating sediment W release into the water column is of considerable ecological and economic significance.

In situ sediment capping represents a principal strategy for suppressing the release of W from contaminated sediments (Chen et al. 2022; Chen et al. 2023; Chen et al. 2024a; Li et al. 2024a; Li et al. 2024b; Chen et al. 2025a). La-modified bentonite (LMB) capping primarily immobilizes W through complexation between La^{3+} and WO_4^{2-} (Chen et al. 2022; Chen et al. 2024a; Chen et al. 2025a). Calcium peroxide (CaO_2) capping relies on the complexation of Ca^{2+} with WO_4^{2-} and subsequent adsorption onto in situ formed Fe(III)/Mn(IV) oxyhydroxides to control W release (Chen et al. 2023). Nano-cerium oxide capping can effectively reduce sedimentary W release while also decreasing the content of soluble and labile W fractions (Li et al. 2024a). Similarly, lanthanum carbonate capping inhibits W release by forming stable La–W precipitates (Li et al. 2024b). W exhibits a strong adsorption affinity for iron, followed by manganese (Iwai & Hashimoto 2017). RC, a by-product rich in reactive iron and aluminum oxides (Xie et al. 2013), presents a potential but underexplored material for controlling W release from sediments. However, reports on the use of RC and its modified forms for this purpose remain scarce, highlighting a gap that warrants further investigation.

Therefore, the objectives of this study are: (1) to synthesize LaRC and evaluate its adsorption capacity for W; (2) to apply RC and LaRC for remediating W-contaminated sediments from Yangcheng Lake, using high-resolution sampling techniques coupled with XPS analysis to assess remediation effectiveness and elucidate the underlying mechanisms; and (3) to evaluate the environmental risk of this approach by comparing it with existing remediation materials. We hypothesize that LaRC capping can effectively suppress W release from sediments, providing an

efficient and low-risk technological solution for managing sedimentary W pollution. This study not only proposes a novel method for inhibiting W mobilization from sediments but also contributes to enhance water quality and aquatic resource safety management.

2 Materials & Methods

2.1 Materials preparation and characterization

Lanthanum-modified red clay (LaRC) was synthesized via a liquid-phase method. Pristine red clay (RC) was mixed with a lanthanum chloride solution and agitated in a constant temperature oscillator to facilitate the loading of lanthanum ions onto the clay. Post-reaction, the solid product was collected by centrifugation and thoroughly rinsed with deionized water to eliminate residual ions. The resulting material was then oven-dried, ground, and sieved to obtain the LaRC adsorbent for subsequent experiments. A tungsten (W) stock solution was prepared using tungstate salt and diluted to a series of target concentrations for the adsorption isotherm studies. Batch adsorption experiments were conducted by mixing a fixed mass of RC or LaRC with tungsten solutions of varying concentrations. The mixtures were oscillated at a constant temperature until equilibrium was reached, after which the residual tungsten concentration in the supernatant was determined. To ensure data reliability, all concentration points were tested in triplicate. Detailed experimental parameters are provided in the Supplementary Material (Table S1).

2.2 Adsorption experiments

Water and sediment samples utilized in the incubation experiment were collected from Yangcheng Lake. The collected sediment was homogenized and passed through a sieve to remove coarse particles and macrofauna, ensuring uniformity. The homogenized sediment was then transferred into plexiglass tubes to establish sediment cores with a defined thickness. All sediment cores underwent a pre-incubation period under simulated conditions to stabilize their physicochemical properties prior to the formal capping experiment. Following pre-incubation, a set of homogeneous cores was selected and randomly divided into three groups for the

capping experiment: a control group (no capping material), an RC-capped group, and a LaRC-capped group. The capping materials were carefully and uniformly applied onto the sediment surface. The entire experiment was conducted under controlled temperature conditions. Specific details regarding sampling information, incubation apparatus dimensions, and experimental conditions are available in the Supplementary Material (Table S2).

2.3 Sediment capping experiments

During the capping experiment, vertical profiles of dissolved oxygen (DO) and pH within the sediment were periodically measured using microelectrodes. Subsequently, porewater samples were collected at various depths using HP-Peeper. The collected porewater was analyzed for dissolved iron (Fe(II)), manganese (Mn), and W concentrations. Fe(II) concentration was determined spectrophotometrically using the 1,10-phenanthroline method (Tamura et al. 1974), while W and Mn concentrations were quantified via inductively coupled plasma mass spectrometry (ICP-MS). Based on the measured W concentration gradients across the sediment-water interface, the diffusive flux was calculated according to Fick's first law of diffusion. At the conclusion of the experiment, surface sediment samples were collected, freeze-dried, and subjected to a sequential extraction procedure to analyze the geochemical fractions of tungsten. Furthermore, the LaRC material, both before and after W adsorption, was characterized using X-ray photoelectron spectroscopy (XPS) to elucidate the adsorption mechanism. All sampling time points, specific instrument models, analytical methods, and parameters are detailed in Table S3.

2.4 Data analysis

Adsorption isotherms were fitted to the Langmuir (Langmuir 1916), Freundlich (Freundlich 1926) and Dubinin-Radushkviech (DR) (Tian & Sa saki 2019)equations.

Langmuir equation：

$$q_e = \frac{q_m K_L C_e}{1 + K_L C_e}$$

Freundlich equation：

$$q_e=K_f C_e^{1/n}$$

Dubinin-Radushkviech (DR) equation：

$$q_e=q_{dr}exp\left(-K_{dr}\left(RTln\left(1+\frac{1}{C_e}\right)\right)^2\right)$$

In these equations, Ce (mg L^{-1}) is the equilibrium W concentration in solution, q_e (mg g^{-1}) is the amount adsorbed per unit mass of adsorbent, q_m (mg g^{-1}) is the maximum monolayer adsorption capacity, and K_L (L mg^{-1}), K_f, and $1/n$ are the Langmuir and Freundlich constants, respectively. For the D–R model, q_{dr} (mg g^{-1}) is the theoretical saturation capacity, K_{dr} (mol^2 kJ^{-2}) is a constant related to adsorption energy, R (8.314 J mol^{-1} K^{-1}) is the universal gas constant, T (K) is the absolute temperature, and E (kJ mol^{-1}) is the mean free energy of adsorption. The value of E provides insight into the adsorption mechanism: E<8 kJ/mol indicates physisorption, 8<E<16 kJ/mol suggests ion exchange or ligand exchange processes, and E>16 kJ/mol corresponds to chemisorption(Zaki et al. 2012, Munagapati et al. 2019, Tian & Sasaki 2019, Lin et al. 2020). All statistical analyses were performed using appropriate software, and differences were considered significant at p<0.05.

3 Results and Discussion

3.1 Adsorption performance and mechanism of LaRC for tungsten

Figure 1 illustrated the adsorption isotherms of W onto RC and LaRC, revealing that the adsorbed amount on both materials increased progressively with rising equilibrium concentration. The Langmuir model provided a better description of the adsorption data for both sorbents (Table 1), yielding q_m of 54.73 mg g^{-1} for RC and 83.94 mg g^{-1} for LaRC. The E value calculated from the D–R model constant K_{dr} for W adsorption on RC was 19.27 kJ mol^{-1}, which has exceeded 16.00 kJ mol^{-1}. Based on the E values derived from the D-R model, the adsorption of W onto RC (19.27 kJ mol^{-1}) is consistent with a chemisorption mechanism. In comparison, the lower E value obtained for LaRC (14.73 kJ mol^{-1}) falls between the 8–16 kJ mol^{-1}, implying

199 that ligand exchange governs the adsorption process.

200 The XPS spectra of red mud before and after La^{3+} loading, as well as of LaRC
201 before and after W adsorption, are shown in Figures 2a–d. In the full-scan spectrum
202 of LaRC, a peak assigned to the La 3d orbital was observed, indicating the
203 successful loading of La^{3+} onto RC (Figure 2a). After W adsorption, a new peak
204 attributed to the W 4f orbital appeared in the full-scan spectrum of LaRC, confirming
205 the successful loading of tungstate onto LaRC following contact with the tungstate
206 solution (Figure 2a) (Kumar et al. 2023; Li et al. 2024b). The W 4f peak of LaRC
207 after W adsorption could be deconvoluted into two peaks, consistent with the
208 characteristic peaks of WO_4^{2-} (Figure 2b) (Shanthi et al. 2023; Li et al. 2024b). After
209 tungstate adsorption on LaRC, the position of the La 3d peak shifted slightly (Figure
210 2c), suggesting possible electron transfer within the valence band of La. This implies
211 that La in LaRC serves as the primary binding site for tungstate, and an inner-sphere
212 La–O–W complex is formed during the adsorption process (Hu et al. 2007; Li et al.
213 2024b). Following tungstate adsorption, the O 1s XPS spectrum showed noticeable
214 changes (Figure 2d). Deconvolution results revealed that the O 1s spectrum of LaRC
215 comprises three oxygen species: 532.89 eV (adsorbed H_2O), 531.98 eV (La–OH),
216 and 530.93 eV (La–O–). After tungstate adsorption, the relative content of La–OH +
217 La–O–W at 531.95 eV decreased from 20.83% to 17.16%, and the relative content of
218 La–O– at 531.02 eV decreased from 44.45% to 37.46%. This reduction may rely on
219 the formation of an inner-sphere complex through La–O–W bonding between W and
220 O–La (Wu et al. 2022; Li et al. 2024b).

221 ## 3.2 Effects of LaRC on sediment DO and pH

222 The variations in DO and pH in the sediments were illustrated in Figure 3.
223 When compared with the controls, LaRC capping increased the DO concentration in
224 the overlying water and sediments by 2.71 μmol L^{-1} and 25.17 μmol L^{-1}, respectively,
225 at week 2. In contrast, at weeks 5 and 8, LaRC capping reduced the DO
226 concentrations in both the overlying water and sediments. Specifically, relative to the
227 control, LaRC capping decreased DO in the overlying water by 12.72 μmol L^{-1} at

week 5 and by 17.98 μmol L^{-1} at week 8, while DO in the sediments decreased by 16.48 μmol L^{-1} and 11.56 μmol L^{-1} at weeks 5 and 8, respectively.For the RC treatment, compared with the control, DO in the overlying water decreased by 17.11 μmol L^{-1} at week 2 but increased by 29.63 μmol L^{-1} and 58.43 μmol L^{-1} at weeks 5 and 8, respectively. Regarding sediment DO, RC capping resulted in increases of 6.55 μmol L^{-1} and 11.34 μmol L^{-1} at weeks 5 and 8 relative to the control.

At weeks 2, 5, and 8, the pH of the overlying water showed little variation among the treatment groups. The pH in control group were 8.38, 7.76, and 7.98, respectively; in the RC group they were 8.16, 7.71, and 7.70; and in the LaRC group they were 8.11, 7.66, and 7.54. Compared with the control, RC capping increased sediment pH by 3.00% and 2.80% at weeks 2 and 5, respectively, but decreased it by 9.41% at week 8. Relative to the control, both RC and LaRC capping increased sediment pH at week 2 by 2.16% and 1.56%, respectively; decreased it by 0.65% and 1.36% at week 5; and further decreased it by 3.54% and 5.54% at week 8.

3.3 Effects of LaRC on Sediment Tungsten

Figure 4 demonstrated the temporal changes in soluble W concentrations across different treatment groups. At week 2, no obvious difference was observed in the release of soluble W from sediment between three groups. In contrast, at weeks 5 and 8, both RC and LaRC capping significantly suppressed soluble W levels in the sediment. Specifically, compared to the control, RC capping reduced concentrations by 45.61% (upper 10 cm, week 5) and 21.00% (upper 6.5 cm, week 8). And LaRC capping reduced the soluble W concentration by 56.07% and 32.23% in the upper 10 cm of sediment at weeks 5 and 8, respectively.

The impact of capping on soluble W release flux is depicted in Figure 5. At week 2, both RC and LaRC capping enhanced the flux compared to the control. Conversely, at weeks 5 and 8, both treatments reduced it. RC capping lowered the flux by 0.13 μg m^{-2} d^{-1} (week 5) and 0.15 μg m^{-2} d^{-1} (week 8), and LaRC capping resulted in decreases of 0.98 μg m^{-2} d^{-1} and 0.11 μg m^{-2} d^{-1} at the corresponding time points.

The results of W fractionation are presented in Figure 6. Relative to the control group, RC capping reduced the content of the F1 fraction by 4.28%, and increased the contents of the F2 fraction, F3 fraction , F4 fraction , and F5 fraction by 7.64%, 25.23%, 3.15%, and 9.78%, respectively. In contrast, LaRC capping decreased the contents of the F1 and F5 fractions by 42.53% and 13.22%, respectively, while increasing the contents of the F2, F3, and F4 fractions by 24.21%, 6.64%, and 6.92%, respectively.

3.4 Effects of LaRC capping on soluble Fe(II) and Mn in sediments

The effects of capping on soluble Fe(II) and Mn are shown in Figure 7. At week 2, both LaRC and RC capping increased the concentrations of these elements in the sediment relative to the control. However, at weeks 5 and 8, the treatment groups diverged: LaRC capping maintained elevated levels, whereas RC capping reduced them. The decreases due to RC capping reached 0.25 mg L^{-1} (week 5) and 0.91 mg L^{-1} (week 8) for soluble Fe(II) in the upper 10 cm, and 0.29 mg/L (week 5) and 0.14 mg/L (week 8) for soluble Mn.

Pearson correlation analysis revealed significant positive associations between soluble W and both Fe(II) and Mn in the control and RC groups (Table 2). A similar trend was observed in the LaRC group, with one exception: the correlation between soluble W and Fe(II) was not significant at week 5 ($p < 0.05$).

3.5 Mechanism of LaRC Capping in Remediating Tungsten-Contaminated Sediments

The suppression of soluble W release by RC capping was evidenced by the reduced concentrations in pore water and decreased fluxes at weeks 5 and 8 (Figs. 4 & 5). This immobilization effect is attributed to the transformation of W into more stable geochemical forms, suggested by the decreased F1 fraction and increased F3 and F4 fractions following capping (Fig. 6). The underlying mechanism likely involves precipitation with iron/aluminum oxides, kaolinite, and hydromica present

285 in the capping material (Xie et al. 2013), a hypothesis supported by DR model
286 analysis of RC before and after W adsorption (Fig. 1 and Table 2). For LaRC
287 capping, the reduced soluble W concentration in pore water and its diminished
288 release flux at weeks 5 and 8 demonstrate that a passivation layer formed on the
289 sediment surface effectively blocked the upward migration of soluble W (Figs. 4 and
290 5). The decrease in the F1 fraction and the concurrent increases in the F3 and F4
291 fractions under LaRC treatment indicate that LaRC promotes the transformation of
292 labile W into stable forms, thereby enhancing the sediment's immobilization
293 capacity for W (Fig. 6). The dominant mechanism for controlling W release by
294 LaRC is attributed to the formation of La–W precipitates (e.g., $La_2(WO_4)_3$) (Figs. 1
295 and 2; Table 1) (Chen et al. 2022, Li et al. 2024b). These precipitates result from the
296 reaction between La^{3+} in LaRC and tungstate ions, as evidenced by DR model fitting
297 and XPS analysis of LaRC before and after W adsorption (Figs. 1 and 2; Table
298 1) (Chen et al. 2022; Li et al. 2024b).

299 The strong positive correlations between soluble W and both Fe(II) and Mn
300 (Table 2) underscore the pivotal role of iron and manganese in regulating W release
301 from sediments (Iwai & Hashimoto 2017; Wasylenki et al. 2020; Chen et al. 2024a;
302 Lin et al. 2024; Chen et al. 2025a). Under RC treatment, the observed decline in
303 soluble Fe(II) and Mn is attributed to enhanced DO infiltration into the sediment,
304 which promotes the oxidation of adsorbed Fe(II) and Mn(II) on RC surfaces,
305 forming Fe(III)/Mn(IV) oxyhydroxides (Figs. 3 & 7). In contrast, the progressive
306 accumulation of soluble Fe(II) and Mn under LaRC treatment suggests enhanced
307 reductive dissolution of Fe(III)/Mn(IV) oxyhydroxides (Fig. 7). Nevertheless,
308 despite this release, soluble W does not accumulate, likely due to the strong affinity
309 between La^{3+} and WO_4^{2-}, leading to the formation of insoluble La–W precipitates.
310 This mechanism is corroborated by DR model and XPS analyses of LaRC before
311 and after W adsorption (Figs. 1, 2 and Table 1) (Chen et al. 2022; Li et al. 2024b;
312 Chen et al. 2025a), explaining the apparent paradox of rising Fe(II)/Mn alongside
313 declining W concentrations under LaRC treatment (Chen et al. 2024a; Chen et al.

2025a)。

3.6 Environmental Benefits Assessment of LaRC Capping

This study demonstrated that LaRC capping not only effectively immobilizes soluble W but also reduces its diffusive flux across the sediment-water interface. Additionally, La-oxides are resistant to reduction, and their complexes with W (W–La-oxides) are more stable under reducing conditions compared to W conventionally bound to Fe(III)/Mn(IV) oxyhydroxides. A further comparison was made between LaRC and RC, as well as other currently reported capping materials, such as lanthanum-modified bentonite (LMB) (Chen et al. 2022; Chen et al. 2025a), lanthanum carbonate (LC)(Li et al. 2024b), cerium oxide nanoparticles (CNP) (Li et al. 2024a) and calcium peroxide (CP) (Chen et al. 2023) , regarding their performance in remediating sedimentary W.The adsorption capacity of LaRC (83.94 mg/g) is higher than that of RC (54.7 mg g^{-1}), LMB (52.8 mg g^{-1}) (Chen et al. 2022), CNP (58.1 mg g^{-1}) (Li et al. 2024a), CP (46.1 mg g^{-1}) (Chen et al. 2023), and LC (25.3 mg g^{-1}) (Li et al. 2024b).In terms of remediation efficacy, LaRC capping achieved the greatest reduction in the diffusive flux of soluble W (0.98 μg m^{-2} d^{-1}), which is notably higher than the reductions achieved by RC (0.15 μg m^{-2} d^{-1}), LMB (0.23 μg m^{-2} d^{-1}), CNP (0.3 μg m^{-2} d^{-1}), CP (0.42 μg m^{-2} d^{-1}), and LC (0.76 μg m^{-2} d^{-1}). The immobilization efficiency for soluble W in pore water by LaRC capping (56.1%) was second only to LC (68.5%) and CNP (60.1%), but higher than RC (45.6%), LMB (45.8%), and CP (43%). The dosage of LaRC used (3.0 g) was only higher than that of CNP (0.05 g) but lower than LMB (5.5 g), LC (20 g), and CP (10 g). Compared to other materials, LaRC exhibits a significant advantage in W adsorption capacity and demonstrates competitive remediation performance for sedimentary W even at a lower application dosage. However, LaRC capping showed minimal control over sedimentary W in the initial stages of the experiment. Therefore, further optimization of the modification method and validation of its capping effectiveness are required before LaRC can be applied in practical scenarios.

4 Conclusion

In this study, a novel capping material, LaRC, was developed for controlling the release of W from contaminated sediments. The results indicated that LaRC exhibits a high adsorption capacity for W. Relative to unmodified RC, LaRC exhibits superior performance in immobilizing soluble W within sediment pore water and simultaneously reducing its diffusive flux across the sediment-water interface. Moreover, the La-W oxyhydroxides formed during the LaRC capping process demonstrate greater stability under reducing conditions compared to those associated with Fe(III)/Mn(IV) oxyhydroxides, thereby lowering the potential for W remobilization. Overall, LaRC shows excellent adsorption capability and effective remediation performance for W-contaminated sediments. This study demonstrate the considerable potential of LaRC for remediating W-contaminated sediments and offer a scientific foundation for managing tungsten in aquatic ecosystems.

Conflicts of Interest

The authors state that there is no conflict of interest on their part with any individual or organization.

Author contributions

Hanxiao Wang, Writing original draft, Formal analysis, Data curation, Investigation; Jiabao Yan, Software, Project administration, Supervision, Formal analysis; Li Zhou, Methodology; Dongdong Zhu, Formal analysis; Qi Li, Methodology; Yan Wang, Formal analysis; Jing Xiao, Project administration, Methodology; Lan Zhang, Methodology; Xiaohui You, Formal analysis; Xiang Chen, Writing-review and editing, Funding acquisition, Supervision, Methodology; Xiaoshuai Hang, Funding acquisition, Project administration, Conceptualization.

Acknowledgements

This research was financially supported by the National Natural Science Foundation of China (42407557), the Project of Ecological and Environmental

Protection Integration Research Institute in Yangtze River Delta (ZX2023SZY118) and the Special Basic Research Service for the Central Level Public Welfare Research Institute (GYZX250105)).

References

Adamakis I-DS, Panteris E, Eleftheriou EP (2012) Tungsten Toxicity in Plants. Plants (Basel) 1: 82-99, https://doi.org/10.3390/plants1020082

Bolt AM, Mann KK (2016) Tungsten: an Emerging Toxicant, Alone or in Combination. Curr Environ Health Rep 3: 405-415, https://doi.org/10.1007/s40572-016-0106-z

Bostick BC, Sun J, Landis JD, Clausen JL (2018) Tungsten Speciation and Solubility in Munitions-Impacted Soils. Environ Sci Technol 52: 1045-1053, https://doi.org/10.1021/acs.est.7b05406

Chen X, Liu L, Yan W, Li M, Guo Z, Li Q, He X, Zhao Z, Liu R, Zhang S, Huang Y, Jiang F (2022) Effect of lanthanum modified bentonite capping on control of sediment phosphorus and tungsten release. Ecol Eng 185: 106788, https://doi.org/10.1016/j.ecoleng.2022.106788

Chen X, Liu L, Yan W , Li M, Li Q, He X, Zhao Z, Liu R, Zhang S, Huang Y, Jiang F (2023) Impacts of calcium peroxide on phosphorus and tungsten releases from sediments. Environ Res 231: 116060, https://doi.org/10.1016/j.envres.2023.116060

Chen X, Liu L, Wang Y, Zhou L, Xiao J, Yan W, Li M, Li Q, He X, Zhang L, You X, Zhu D, Yan J, Wang B, Hang X (2024a) The combined effects of lanthanum-modified bentonite and Vallisneria spiralis on phosphorus, dissolved organic matter, and heavy metal(loid)s. Sci Total Environ 917: 170502, https://doi.org/10.1016/j.scitotenv.2024.170502

Chen X, Wang Y, Zhang L, Zhu D, Yan W, Li M, Jin J, Wu T, Li Q, He X, Wu G, Tian Y, You X, Yan J, Xiao J, Zhou L, Hang X (2024b) Tungsten migration and transformation characteristics in lake sediments under changing habitats from

algae to macrophytes. J Hazard Mater 480: 136134, https://doi.org/10.1016/j.jhazmat.2024.136134

Chen X, Li M, He X, Li Q, Jin J, Wu T, Shao Y, Wu J, Li G, Wang Y, Yan W (2025a) Behavior of iron and manganese in lanthanum-modified bentonite and calcium peroxide passivated sediments and the coupling effect on cobalt and tungsten. J Environ Chem Eng 13(5), 117684, https://doi.org/10.1016/j.jece.2025.117684

Chen X, Wang Y, Li M, He X, Li Q, Jin J, Wu T, Shao Y, Wu J, Li G, Liu L, Yan W (2025b) Seasonal changes-facilitated release of phosphorus and tungsten from the Lake Taihu sediments through reductive dissolution of Fe/Mn (hydr)oxides and competitive adsorption with dissolved organic matter. Environ Pollut 383: 126745, https://doi.org/10.1016/j.envpol.2025.126746

Du H, Xu Z, Hu M, Zhang H, Peacock CL, Liu X, Nie N, Xue Q, Lei M, Tie B (2020) Natural organic matter decreases uptake of W(VI), and reduces W(VI) to W (V), during adsorption to ferrihydrite. Chem Geol 540: 119567, https://doi.org/10.1016/j.chemgeo.2020.119567

Du H, Li Y, Wan D, Sun C, Sun J (2022) Tungsten distribution and vertical migration in soils near a typical abandoned tungsten smelter. J Hazard Mater 429: 128292, https://doi.org/10.1016/j.jhazmat.2022.128292

Freundlich H (1926) Colloid and Capillary Chemistry (Freundlich, Herbert). J. Chem Educ 3: 1454, https://doi.org/10.1021/ed003p1454.2

Gold K, Cheng Y, Holmes TD (2007) A quantitative analysis of aerosols inside an armored vehicle perforated by a kinetic energy nickel, penetrator containing tungsten, and cobalt. Mil Med 172: 393-398, https://doi.org/10.7205/milmed.172.4.393

Grant MP, VanderSchee CR, Chou H, Bolt A, Epure LM, Kuter D, Antoniou J, Bohle S, Mann KK, Mwale F (2021) Tungsten accumulates in the intervertebral disc and vertebrae stimulating disc degeneration and upregulating markers of inflammation and pain. Eur Cell Mater 40: 517-530, https://doi.org/10.22203/eCM.v041a33

Guan D, Williams PN, Xu H, Li G, Luo J, Ma L (2016) High-resolution

measurement and mapping of tungstate in waters, soils and sediments using the low-disturbance DGT sampling technique. J Hazard Mater 316: 69-76, https://doi.org/10.1016/j.jhazmat.2016.05.026

Hadrup N, Sorli JB, Sharma AK (2022) Pulmonary toxicity, genotoxicity, and carcinogenicity evaluation of molybdenum, lithium, and tungsten: A review. Toxicology 467: 153098, https://doi.org/10.1016/j.tox.2022.153098

Hu C, Liu H, Dong W, Zhang Y, Bao G, Lao C, Wang Z (2007) $La(OH)_3$ and La_2O_3 nanobelts-Synthesis and physical properties. Adv Mater 19: 470-474, https://doi.org/10.1002/adma.200601300

Iwai T, Hashimoto Y (2017) Adsorption of tungstate (WO_4) on birnessite, ferrihydrite, gibbsite, goethite and montmorillonite as affected by pH and competitive phosphate (PO_4) and molybdate (MoO_4) oxyanions. Appl Clay Sci 143: 372-377, https://doi.org/10.1016/j.clay.2017.04.009

Kashiwabara T, Takahashi Y, Marcus MA, Uruga T, Tanida H, Terada Y, Usui A (2013) Tungsten species in natural ferromanganese oxides related to its different behavior from molybdenum in oxic ocean. Geochim Cosmochim Acta 106: 364-378, https://doi.org/10.1016/j.gca.2012.12.026

Kelly ADR, Lemaire M, Young YK, Eustache JH, Guilbert C, Molina MF, Mann KK (2013) In Vivo Tungsten Exposure Alters B-Cell Development and Increases DNA Damage in Murine Bone Marrow. Toxicol Sci 131: 434-446, https://doi.org/10.1093/toxsci/kfs324

Kumar KN, Vijayalakshmi L, Lim J, Choi J (2023) Dazzling green luminescent and biocompatible Tb3+-activated lanthanum tungstate nanophosphors for group-III evaluation of latent fingerprints and anticancer applications. J Alloys Compd 959: 170415, https://doi.org/10.1016/j.jallcom.2023.170415

Langmuir I (1916) The constitution and fundamental properties of solids and liquids part I. solid. J Am Chem Soc 38: 2221–2295, https://doi.org/10.1021/ja02268a002

Li Q, Liu L, Yan W, Chen X, Liu R, Zhao Z, Jiang F, Huang Y, Zhang S, Zou Y, Yang C (2024a) Influence on the release of arsenic and tungsten from sediment,

and effect on other heavy metals and microorganisms by ceria nanoparticle capping. Environ Pollut 343: 123161, https://doi.org/10.1016/j.envpol.2023.123161

Li Q, Yan W, Li M, Chen X, Wu T, He X, Yao Q, Yan Y, Li G (2024b) Simultaneous immobilization of sediment internal phosphorus, arsenic and tungsten by lanthanum carbonate capping. Environ Res 242: 117817, https://doi.org/10.1016/j.envres.2023.117817

Li W, Liu G, Lei M, Zhou Y, Cui H, Du H (2025) Spectral fingerprints of DOM-tungsten interactions: Linking molecular binding to conformational changes. J Hazard Mater 483: 136649, https://doi.org/10.1016/j.jhazmat.2024.136649

Lin J, Chen X, Liu Y, Wang Y, Shuai J, Chen M (2024) Fe/Mn (oxyhydr)oxides reductive dissolution promoted by cyanobacterial algal bloom-derived dissolved organic matter caused sediment W release during an algal bloom in Taihu Lake. Water Res 260: 121899, https://doi.org/10.1016/j.watres.2024.121899

Lin J, Wang Y, Zhan Y (2020) Novel, recyclable active capping systems using fabric-wrapped zirconium-modified magnetite/bentonite composite for sedimentary phosphorus release control. Sci Total Environ 727: 138633, https://doi.org/10.1016/j.scitotenv.2020.138633

Lu L, Rao W, Song Y, Lei M, Tie B, Du H (2022) Natural dissolved organic matter (DOM) affects W(VI) adsorption onto Al (hydr)oxide: Mechanisms and influencing factors. Environ Res 205: 112571, https://doi.org/10.1016/j.envres.2021.112571

Miller AC, Mog S, McKinney L, Luo L, Allen J, Xu J, Page N (2001) Neoplastic transformation of human osteoblast cells to the tumorigenic phenotype by heavy metal-tungsten alloy particles: induction of genotoxic effects. Carcinogenesis 22: 115-125, https://doi.org/10.1093/carcin/22.1.115

Miranda LS, Wijesiri B, Ayoko GA, Egodawatta P, Goonetilleke A (2021) Water-sediment interactions and mobility of heavy metals in aquatic

environments. Water Res 202: 117386, https://doi.org/10.1016/j.watres.2021.117386

Munagapati VS, Wen JC, Pan CL, Gutha Y, Wen JH (2019) Enhanced adsorption performance of Reactive Red 120 azo dye from aqueous solution using quaternary amine modified orange peel powder. J Mol Liq 285: 375-385, https://doi.org/10.1016/j.molliq.2019.04.081

Shanthi S, Flower NAL, Sujatha RA, Vinitha G, Rahulan KM (2023) Role of defects on the nonlinear optical properties of La doped Bi2WO6 nanostructures for optical device applications. Opt Mater 136: 113357, https://doi.org/10.1016/j.optmat.2022.113357

Strigul N, Koutsospyros A, Arienti P, Christodoulatos C, Dermatas D, Braida W (2005) Effects of tungsten on environmental systems. Chemosphere 61: 248-258,

Strigul N (2010) Does speciation matter for tungsten ecotoxicology? Ecotox Environ Safe 73: 1099-1113, https://doi.org/10.1016/j.ecoenv.2010.05.005

Tamura H, Goto K, Yotsuyanagi T, Nagayama M (1974) Spectrophotometric determination of iron (II) with 1, 10-phenanthroline in the presence of large amounts of iron (III). Talanta 21: 314-318, https://doi.org/10.1016/0039-9140(74)80012-3

Tian Q, Sasaki K (2019) A novel composite of layered double hydroxide/geopolymer for co-immobilization of Cs^{+} and SeO_4^{2-} from aqueous solution. Sci Total Environ 695: 133799, https://doi.org/10.1016/j.scitotenv.2019.133799

Wang J, Shi D, Ma X, Yang L, Ding S, Liu E (2023) Application of high-resolution techniques in the assessment of the mobility of Cr, Mo, and W at the sediment-water interface of Nansi Lake, China. Environ Monit Assess 195(8): 980, https://doi.org/10.1007/s10661-023-11567-1

Wasylenki LE, Schaefer AT, Chanda P, Farmer JC (2020) Differential behavior of tungsten stable isotopes during sorption to Fe versus Mn oxyhydroxides at low ionic strength. Chem Geol 558: 119836, https://doi.org/10.1016/j.chemgeo.2020.119836

Wu A, Wang Y, Friese K, Zhang L, Han C, Kang D, Shen Q (2021) Spatial and Seasonal Distribution of 2-Methylisoborneol in a Large Eutrophic Shallow Lake, China. Water Air Soil Pollut 232(9): 387, https://doi.org/10.1007/s11270-021-05340-8

Wu D, Zhan Y, Lin J, Zhang Z, Xie B (2022) Contrasting effect of lanthanum hydroxide and lanthanum carbonate treatments on phosphorus mobilization in sediment. Chem Eng J 427: 132021, https://doi.org/10.1016/j.cej.2021.132021

Xie Q, Chen T, Zhou H, Xu X, Xu H, Ji J, Lu H, Balsam W (2013) Mechanism of palygorskite formation in the Red Clay Formation on the Chinese Loess Plateau, northwest China. Geoderma 192: 39-49, https://doi.org/10.1016/j.geoderma.2012.07.021

Xu Z, Liu X, Peng J, Qu C, Chen Y, Zhang M, Liang D, Lei M, Tie B, H. DH (2022) Tungsten–humic substances complexation. Carbon Research 1, 1-12

Zaki AA, El-Zakla T, El Geleel MA (2012) Modeling kinetics and thermodynamics of Cs^{+} and Eu^{3+} removal from waste solutions using modified cellulose acetate membranes. J Membr Sci 401: 1-12, https://doi.org/10.1016/j.memsci.2011.12.044

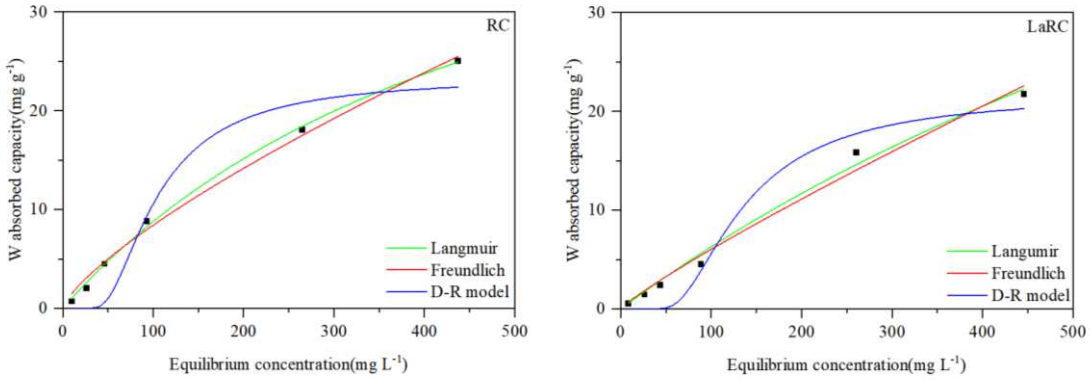


Fig 1 Adsorption isotherms of W on RC and LaRC

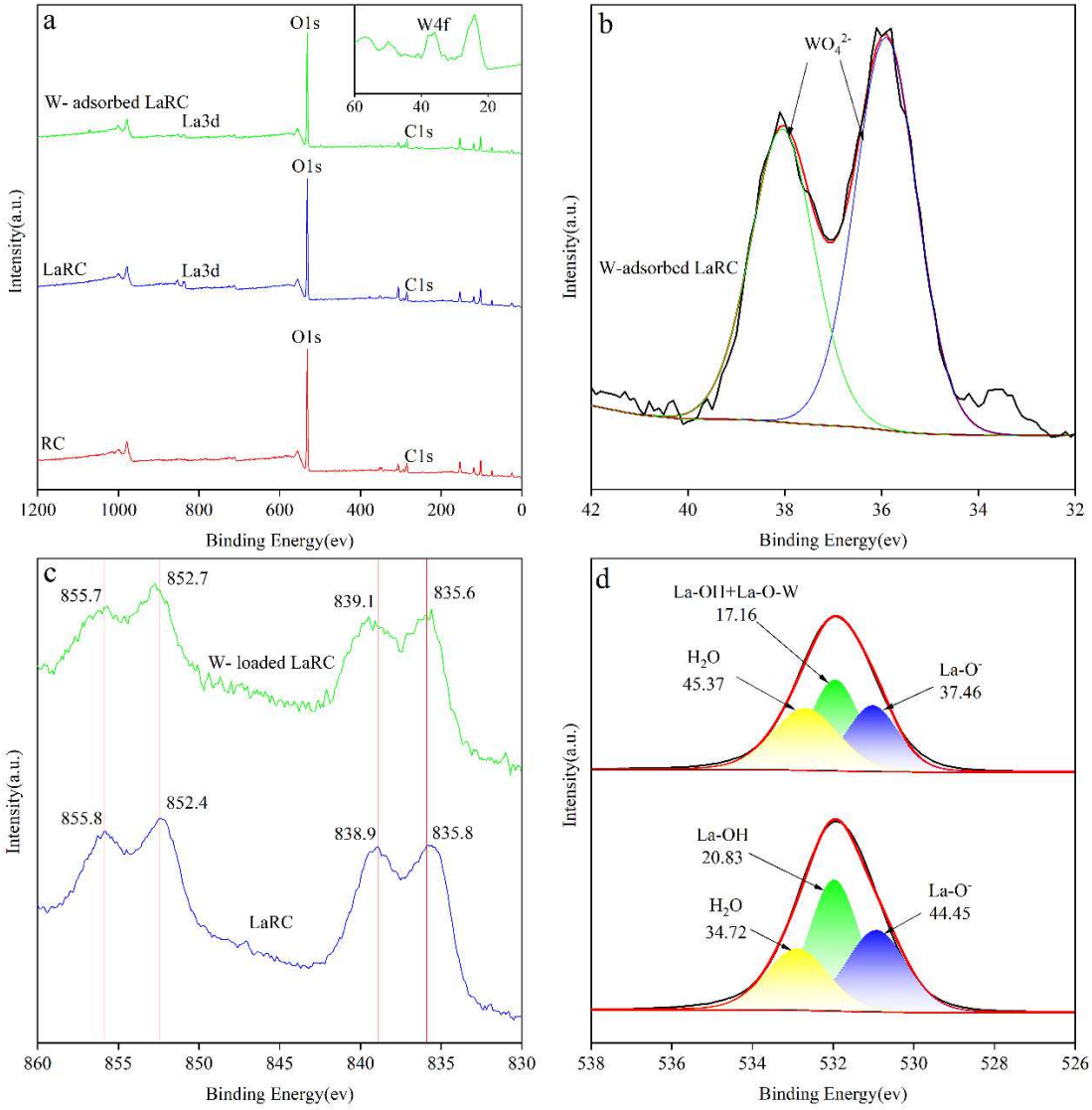


Fig 2 a. XPS full-range spectra of RC before and after La load, and LaRC before and after W adsorption. b. W4f spectrum of LaRC after W adsorption. c and d La 3d and O 1s spectra of LaRC before and after W adsorption.

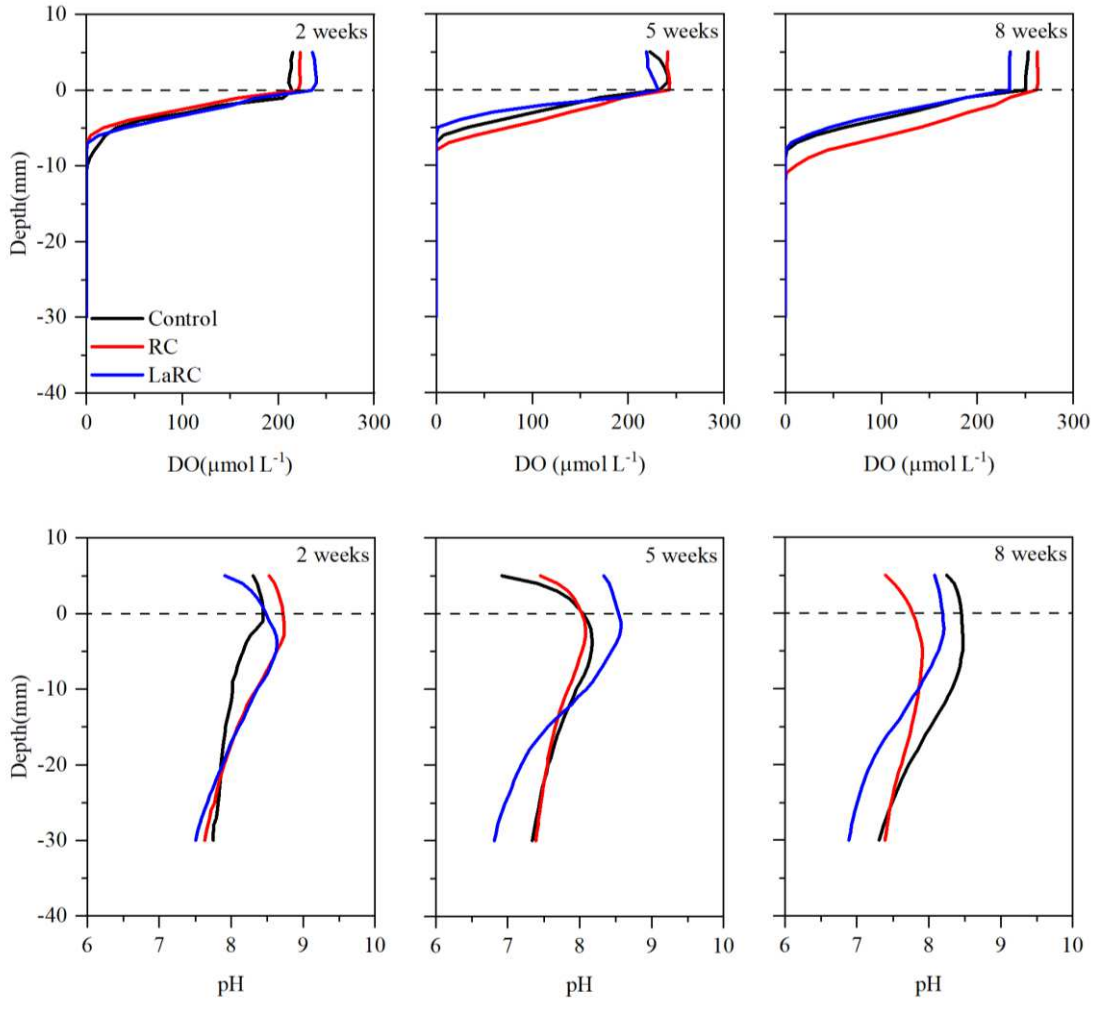


Fig 3 Changes of sediment DO and pH in control, RC, and LaRC treatment groups

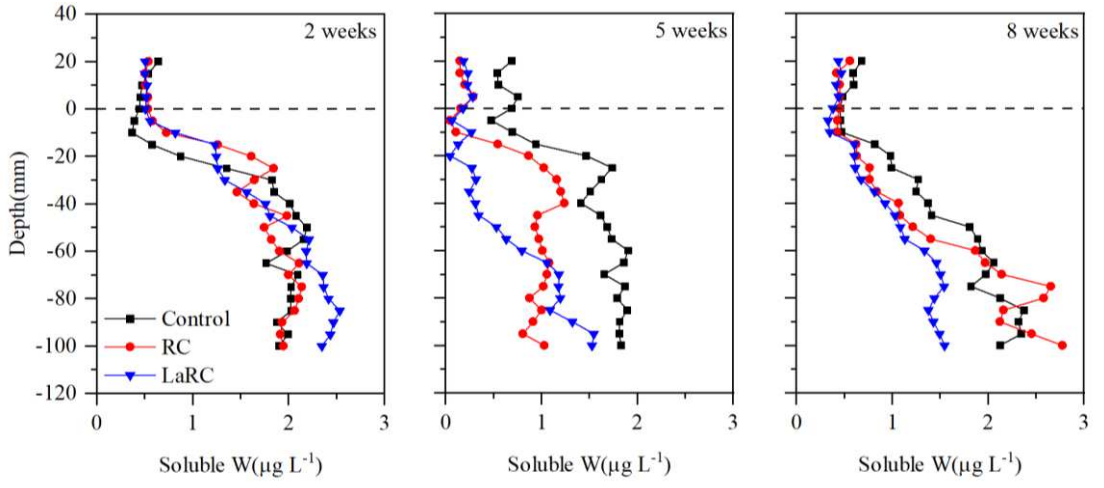
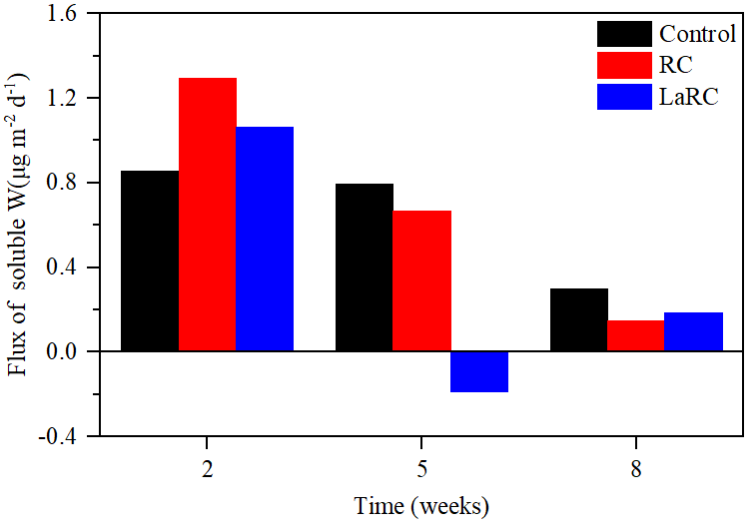


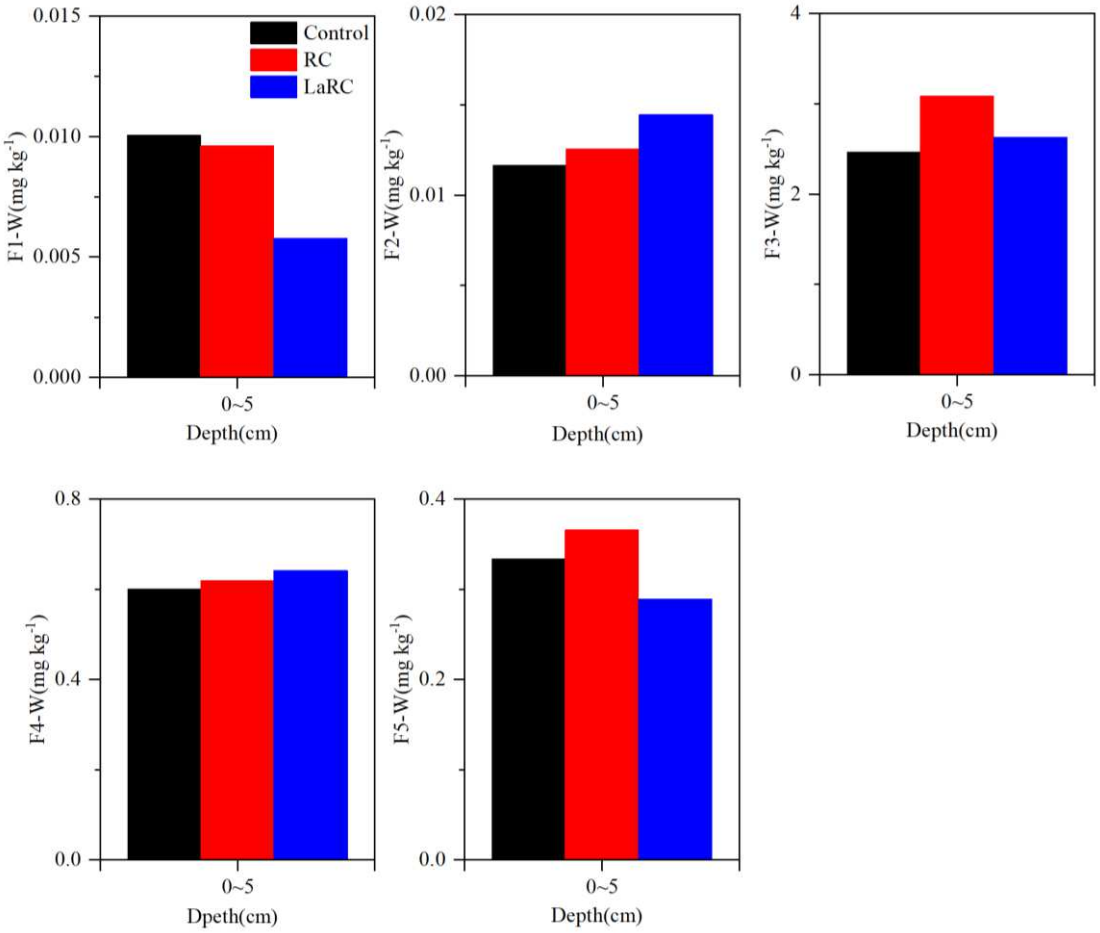
Fig 4 Changes of sediment soluble W in control, RC, and LaRC treatment groups



550

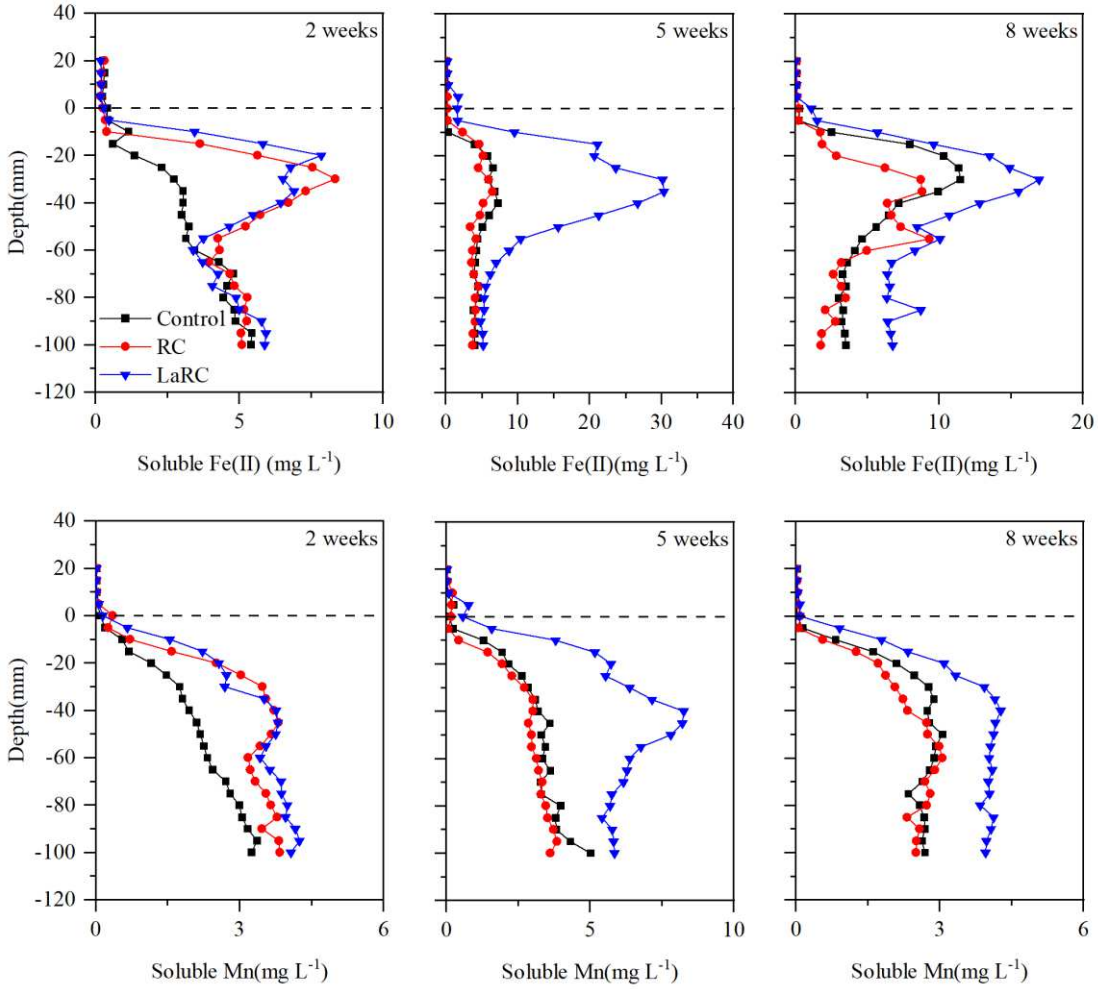
551 **Fig 5** Diffusive fluxes of soluble W across the sediment-water interface (0–20 mm) in control,

552 RC, and LaRC treatment groups



553

554 **Fig 6** Changes of W fractions in surface sediments in control, RC, and LaRC treatment groups



555

556 **Fig 7** Changes of soluble Fe (II) and Mn in control, RC, and LaRC treatment groups

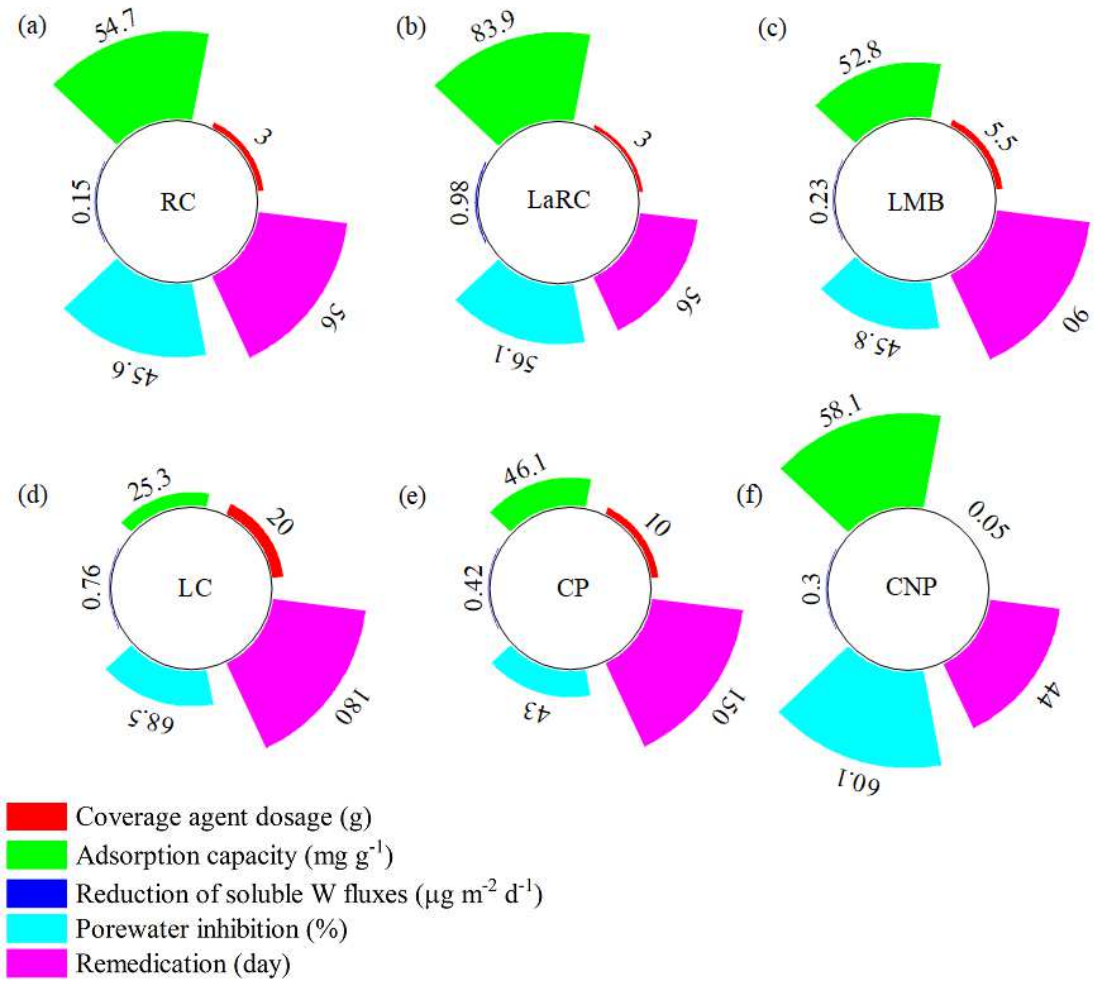


Fig 8 Comparison of Remediation Materials for Tungsten-Contaminated Sediments

561 **Table 1** Langmuir, Freundlich, and D-R model parameters for the sorption of W on RC and

562 LaRC

	RC		LaRC	
Equations	**Parameter**		**Parameter**	
Langmuir	q_m (mg g^{-1})	54.73	q_m (mg g^{-1})	83.94
$q_e = \frac{q_m K_L C_e}{1 + K_L C_e}$	k_f	0.002	k_f	8.09
	R^2	0.998	R^2	0.991
Freundlich	K_f	0.26	K_f	0.10
$q_e = K_f C_e^{1/n}$	n	1.33	n	1.13
	R^2	0.993	R^2	0.986
D-R model	q_m (mg g^{-1})	23.33	q_m (mg g^{-1})	21.67
	β (mol^2 kJ^{-2})	0.0013	β (mol^2 kJ^{-2})	0.0023
$q_e = q_{dr} \exp(-K_{dr}(RT \ln(1 + \frac{1}{C_e}))^2)$	E (kJ mol^{-1})	19.27	E (kJ mol^{-1})	14.73
	R^2	0.926	R^2	0.963

563 **Table 2** Pearson correlations between soluble Fe (II)/Mn and W.

Groups	**Time (weeks)**	**Correlation between W and Fe (II)**		**Correlation between W and Mn**	
		r	p-value	r	p-value
Control	2	0.87**	< 0.001	0.90**	< 0.001
	5	0.79**	< 0.001	0.94**	< 0.001
	8	0.15	0.485	0.83**	< 0.001
RC	2	0.82**	< 0.001	0.96**	< 0.001
	5	0.89**	< 0.001	0.92**	< 0.001
	8	0.09	0.669	0.76**	< 0.001
LaRC	2	0.61**	0.001	0.95**	< 0.001
	5	-0.33	0.104	0.38	0.059
	8	0.23	0.273	0.79**	< 0.001

564 Note: Statistically significant correlations at the levels of $p < 0.05$ and $p < 0.01$ were shown as *

565 and ** , respectively

566

567

Supplementary Files

This is a list of supplementary files associated with this preprint. Click to download.

- Supplementarymaterial.docx